

Select, Hypothesize and Verify: Towards Verified Neuron Concept Interpretation

ZeBin Ji^{†,1}, Yang Hu^{†,1}, Xiuli Bi^{*,1}, Bo Liu¹, Bin Xiao^{1,2}

¹Chongqing Key Laboratory of Image Cognition,
Chongqing University of Posts and Telecommunications, Chongqing, China

²Jinan Inspur Data Technology Co., Ltd., Jinan, China

{S230201044, S210201038}@stu.cqupt.edu.cn, {bixl, boliu, xiaobin}@cqupt.edu.cn

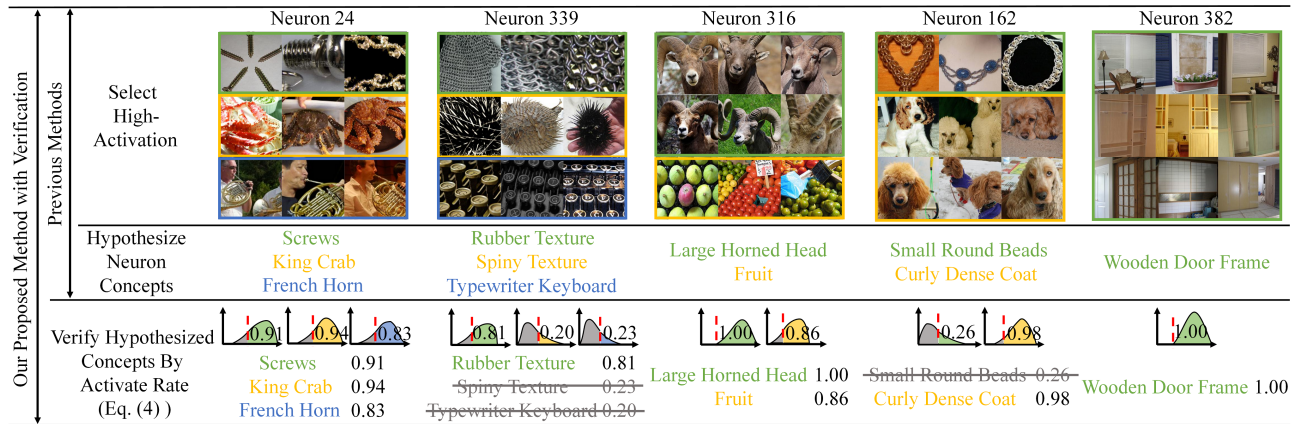


Figure 1. **Comparison of previous methods and our proposed method with verification.** The neurons are sampled from the second-to-last layer of ResNet-18. Existing methods assume that concepts inferred from activated neurons are all accurate, while our proposed method introduces verification to identify incorrect ones. Specifically, for neuron 162, both the concepts (Small Round Beards and Curly Dense Coat) are inferred from high-activation images. Verification shows that the activation rate for small round whiskers (0.26) suggests this concept may be incorrect, while curly dense hair achieves 0.98, confirming the correctness of the concept.

Abstract

It is essential for understanding neural network decisions to interpret the functionality (also known as concepts) of neurons. Existing approaches describe neuron concepts by generating natural language descriptions, thereby advancing the understanding of the neural network’s decision-making mechanism. However, these approaches assume that each neuron has well-defined functions and provides discriminative features for neural network decision-making. In fact, some neurons may be redundant or may offer misleading concepts. Thus, the descriptions for such neurons may cause misinterpretations of the factors driving the neural network’s decisions. To address the issue, we introduce a verification of neuron functions, which checks whether the generated concept highly activates the corresponding neuron. Furthermore, we propose a Se-

lect–Hypothesize–Verify framework for interpreting neuron functionality. This framework consists of: 1) selecting activation samples that best capture a neuron’s well-defined functional behavior through activation-distribution analysis; 2) forming hypotheses about concepts for the selected neurons; and 3) verifying whether the generated concepts accurately reflect the functionality of the neuron. Extensive experiments show that our method produces more accurate neuron concepts. Our generated concepts activate the corresponding neurons with a probability approximately 1.5 times that of the current state-of-the-art method.

1. Introduction

Deep neural networks (DNNs) have achieved remarkable progress in various domains. However, due to their complex structures, understanding the decision-making process of DNNs remains challenging. This opacity not only undermines trust in the models but also limits their deployment in

[†]These authors contributed equally

^{*}Corresponding Author

safety-critical applications. To address this issue, explainable artificial intelligence (XAI) has emerged, aiming to reveal the internal mechanisms of neural networks and make their decision processes transparent and comprehensible.

Previous studies have attempted to break down convolutional neural networks (CNNs) into interpretable neurons, using the visualization techniques [14, 23, 32, 33, 35] (e.g., Saliency Maps [32] and Grad-CAM [30]) to understand models from the most fundamental neurons (also called units, filters, or features). Visualization techniques help to reveal the functions reflected by neurons, but noisy activation can make them challenging to interpret without manual inspection. To address this limitation, researchers have begun describing the functionality of neurons (also referred to as concepts) using natural language, such as Network Dissection [3] and Compositional Explanations [17]. Network Dissection constructs the Broden probe dataset to establish correspondences between visualizations and predefined concepts, while Compositional Explanations extends this approach to generate complex concept compositions. CLIP-Dissect [22] further leverages OpenAI’s CLIP [27] model to achieve more flexible matching.

These works analyze the entire network, providing functional descriptions of neurons in layers close to the input that primarily focus on visual features, such as color and texture. Although these features are indispensable for the model’s decision-making, they contribute only to a limited extent to human understanding of the neural network. Consequently, subsequent research has shifted attention toward neurons in the penultimate layer, whose functions are more aligned with human-understandable concepts. For example, FALCON [11] focuses exclusively on the final layer, removing spurious descriptions by contrasting low-level activations with the corresponding images. Following FALCON, WWW [1] improves the accuracy of neuron descriptions by integrating activation locations and contributions to predictions. DnD [2] uses large language models to generate natural language descriptions, providing higher-quality concepts for neurons.

Although these methods aim to describe neuron functionality accurately, they all rely on the same assumption: that each neuron has a well-defined function and provides discriminative features for neural network decision-making. However, existing studies [6, 19] have shown that networks contain redundant neurons that do not contribute to decisions. Describing such neurons may be misleading by interpreting noisy activations as meaningful functionality, thereby misleading human understanding of neural network decision mechanisms. Moreover, current approaches typically infer neuronal functions based on their activation distributions across probe datasets, essentially involving an observational hypothesis process. However, due to the limited coverage of probe data, these hypotheses may be subject to

dataset biases and may not accurately reflect the roles of the neurons. Therefore, we argue that intervention-based experiments are necessary to validate these hypotheses.

This principle aligns with scientific methodology: scientific understanding arises not only from observation but also from formulating hypotheses and validating them through controlled experiments [25, 26]. For a long time, neuroscience research has followed an “Observe–Hypothesize–Verify” paradigm: researchers first record neural activity to identify neurons associated with specific functions (observation and localization); then propose functional hypotheses based on response patterns (hypothesis); and finally verify the causal role of these neurons in behavior or cognition through controlled experiments (verification). This closed-loop logic has driven progress in fields such as the visual and language cortices, providing a reliable methodology for understanding the brain.

Similarly, we would argue that research into the interpretability of deep neural networks should adhere to the same scientific logic. Inspired by this idea, we propose a Select–Hypothesize–Verify (SIEVE) framework for interpreting neuron functionality. The framework consists of: 1) Select: Identify data samples that consistently elicit high activation for a given neuron based on its activation distribution over the probe dataset; 2) Hypothesize: formulate hypotheses about the neuron’s functional role using these consistently high-activation samples; 3) Verify: conduct intervention experiments on the neuron to assess the strength of the association between the hypothesized concepts and the neuron’s function, thereby ensuring that the hypotheses reliably reflect the internal mechanisms of the neural network. Our main contributions are as follows:

- Existing methods are limited by the assumption that concepts extracted from visual data by large models must be accurate. To mitigate this issue, we propose a Select–Hypothesize–Verify framework for interpreting neuron functionality (dubbed SIEVE), achieving closed-loop verification to remove mismatched concepts.
- This paper demonstrates that some neurons may not provide discriminative features for neural network decision-making. We design a neural filtering mechanism to prevent the introduction of erroneous concepts.
- Extensive experiments validate the effectiveness of our framework, and the generated concepts activate the corresponding neurons with a probability close to 1.5× that of the current state-of-the-art method.

2. Related Works

Visualization. Interpretability is defined as the ability to provide explanations that are understandable to humans. [7, 34]. Early studies mainly achieved this goal through visualization techniques. Representative methods include Saliency Maps [32] and Grad-CAM [30], which highlight

the regions most important for predictions by computing the gradient of the network output with respect to the input pixels. This helps humans to understand which parts of the input the model focuses on. Additionally, activation maximization [16, 20, 23] optimizes the input image to maximize the activation of a neuron, thereby revealing its functionality. Although visualization aids human understanding of neural networks, manual inspection is typically required to determine whether the visualization results are reasonable.

Natural Language Explanations. To provide more explicit explanations, researchers have begun to describe neuron functionality in natural language. Network Dissection [3] pioneered this direction by constructing Broden, a pixel-wise annotated dataset, and establishing correspondences between neurons and concepts through the intersection over union score (IoU) of neuron activation maps and concept segmentation maps. Subsequently, Bau et al. [4] utilized segmentation models to automatically annotate datasets; however, the concept set remained limited by the capacity of pre-trained segmentation models. MILAN [10] trained image-to-text models to generate unrestricted descriptions. CLIP-Dissect [22] and FALCON [11] further utilized CLIP to describe neuron functionality without annotations. In contrast, DnD [2] employed multimodal models to produce more complex natural language descriptions. Bills et al. [5] proposed using LLMs to predict neuron activations of input. MAIA [31] introduced a multimodal agent that autonomously composes API-based tools to conduct iterative experiments for interpreting neurons in vision models. These methods focus on highly activated neuron samples, ignoring the possibility that such activations may merely correspond to average levels and that the neurons may not have well-defined functions. Although Rosa et al. [12] and Oikarinen & Weng. [21] attempted to provide a more comprehensive description of each neuron by subdividing activation ranges, low activation may lead to ambiguous interpretations. By contrast, we focus not only on highly activated samples but also consider whether the neurons provide discriminative features for decision-making.

Intervention-Based Verification. Intervention-based verification methods typically investigate the causal relationship between internal representations and final model decisions by actively modifying input samples or the internal state of the model, such as the output of a single neuron. Early works, such as LIME [28] and Zeiler &ergus. [33], applied local perturbations in the input space to assess the impact of different image regions on model predictions. Morcos et al. [15] further conducted interventions within the network by setting neuron activations to zero, analyzing the importance of individual neurons for model performance. However, these intervention-based verification approaches primarily aim to identify which inputs or neurons the model relies on, and do not evaluate whether

natural language descriptions accurately correspond to the functionality of these neurons. Consequently, they cannot answer whether a neuron truly encodes the intended concept. To address this limitation, we propose an intervention verification method driven by hypothesized concepts. This approach involves constructing input samples based on hypothesized concepts, and then evaluating the consistency between these concepts and the true functionality of neurons by carrying out targeted interventions and observing changes in neuron activation.

3. Method

Our goal is to identify and verify neurons in deep neural networks that possess well-defined functions, thereby enabling humans to understand the decision-making mechanisms of these networks better. Previous studies have shown that the semantics encoded by neurons in the penultimate layer [11] can be interpreted by humans. Therefore, our analysis primarily focuses on the functionality of neurons in these layers. Motivated by scientific methodology, we present a three-stage framework for neuron interpretation and verification (see Fig. 2 for an overview). The framework consists of three key stages: select samples with consistently high activation (Section Sec. 3.2), generate concept hypotheses from the selected samples (Section Sec. 3.3), and verify the hypothesized concepts (Section Sec. 3.4).

3.1. Definitions

Definition 1 (Neuron Activation). Given a pretrained classification network f and an input image x , the activation value of the i -th neuron in layer l is denoted as $a_i^l(x)$. This value measures the response strength of the neuron when processing the input image.

Definition 2 (Neuron Activation Distribution). For a probe dataset \mathcal{D}_{probe} , the activation distribution of neuron i is defined as the set $\{a_i^l(x) \mid x \in \mathcal{D}_{probe}\}$. It describes how the neuron responds to different images in the dataset.

3.2. Select High-Activation Samples

We use a sample-selection mechanism to identify neuron samples that are most indicative of well-defined functional roles. As shown in Fig. 3, this method distinguishes high-discrimination neurons (e.g., Neuron 507) with consistent activation patterns from low-discrimination neurons (e.g., Neuron 144) with scattered responses. Specifically, based on Sec. 3.1, we can obtain the activation distribution of neuron i over the probe dataset \mathcal{D}_{probe} . We then calculate the ratio of the 99-th percentile to the median of this distribution to quantify the neuron’s response. A higher ratio indicates that the neuron exhibits high activation in response to specific stimuli and low activation in response to non-preferred stimuli. According to the activation distribution of neurons, we define a threshold β . If a neuron’s

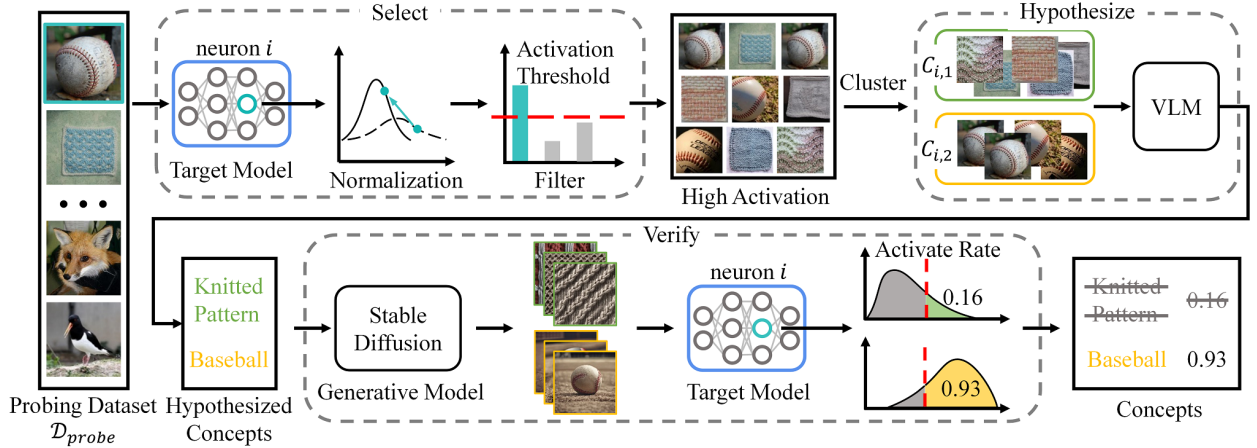


Figure 2. **Overview of SIEVE.** 1) Select: For each sample, we obtain the normalized activation of neuron i from the network’s penultimate layer. Samples with activations above a predefined threshold are identified as high-activation samples. 2) These high-activation samples are clustered, and a vision-language model is used to generate the hypothesized concepts for each cluster. 3) Each concept is converted into a semantic image using text-to-image generation. The generated images are fed into the target model to measure the activation rate of neuron i , thereby verifying the semantic features that the neuron reliably encodes.

ratio exceeds this threshold, it can be considered to encode distinct, well-defined functional features. Through this step, we construct a high-quality set of candidate samples $\mathcal{D}_i^{high} = \{x_1, \dots, x_k\}$, which is used in subsequent hypothesis and verification stages. We select the top 20 samples for each neuron, striking a balance between capturing meaningful neural responses and ensuring computational efficiency.

3.3. Hypothesize Concepts

This stage aims to formulate hypotheses for the candidate sample set \mathcal{D}_i^{high} , describing the potential functional roles. It consists of two steps: high-activation images are clustered to identify distinct functional patterns, and precise concept hypotheses are independently generated for each cluster.

Cluster. For neuron i , a set of highly activated samples \mathcal{D}_i^{high} is obtained as described in Sec. 3.2. To focus on the regions genuinely responsive to the neuron, each sample is cropped according to the neuron’s activation map, yielding a corresponding set of image patches $P_i^{high} = \{p_1, \dots, p_k\}$, where each p_j represents the local region with the highest activation value on the map. This procedure effectively removes irrelevant background, ensuring that the subsequent feature distribution better reflects the neuron’s true function. Feature vectors are then extracted from the set of image patches P_i^{high} , resulting in a feature set $V_i^{high} = \{v_1, \dots, v_k\}$. The feature set V_i^{high} is then clustered to reveal the multiple potential functions a single neuron may correspond to. Specifically, agglomerative clustering [18] is applied to group the feature vectors extracted from the high-activation patches, with the number of clusters being automatically determined by the Silhouette score [29], which evaluates the compactness and separability of the clusters.

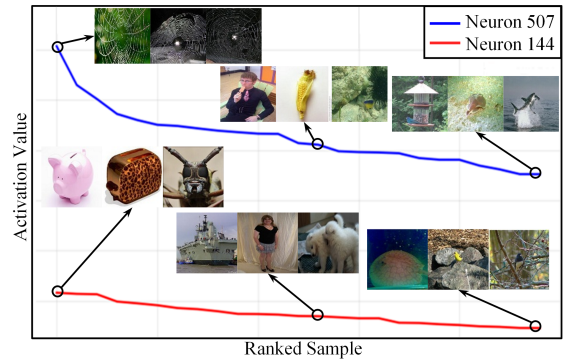


Figure 3. Activation distributions and Concepts of high-discrimination neurons (Neuron 507) and low-discrimination neurons (Neuron 144). The high activation of high-discrimination neurons exhibits consistent patterns while the high activation of low-discrimination neurons fails to do so.

The clustering results partition the high-activation image patches into m clusters $\{C_{i,1}, \dots, C_{i,m}\}$, where $C_{i,j}$ represents the j -th typical response pattern of neuron i .

Hypothesize. To describe each cluster $C_{i,j}$, we follow CLIP-Dissect [22] and introduce a predefined concept set $\mathcal{D}_{concept}$ as $\mathcal{T} = \{t_1, \dots, t_n\}$. We introduce a vision-language model (e.g., CLIP), employing its image encoder $E_I(\cdot)$ and text encoder $E_T(\cdot)$ to project images and texts into a shared embedding space. For each high-activation image patches $x_p \in C_{i,j}$ and each concept $t_q \in \mathcal{T}$, their similarity is calculated as:

$$s(x_p, t_q) = \text{sim}(E_I(x_p), E_T(t_q)) \quad (1)$$

where $\text{sim}(\cdot, \cdot)$ denotes cosine similarity. The matching

	Neuron 662	Neuron 1801	Neuron 91	Neuron 1251	Neuron 1889
Selecting Activation in ResNet-50					
SIEVE(Ours)	Sock, Knitted Pattern Heel Strap, Wear Shoe Displays, Shelves of Shoes	Beer Glass, Liquid Consistency Finely Strained Broth, Soup	Curly dense coat, Irish water spaniel	Pool Table, Pool Concert, Theater	Torch, Candle Dog, Greater Swiss Mountain Dog Tennis, Stick Protruding From Center
CLIP-Dissect	Shoe Shop, Red	Bubbly, Orange	Sheep, Pink	Pool Table, Top	Dog, Orange
WWW	Grid, Footwear	Ingredients, Meat	Dog, Floor	Yellow, Wood	Display, Pot
	Neuron 37	Neuron 361	Neuron 344	Neuron 752	Neuron 183
Selecting Activation in ViT-B/16					
SIEVE(Ours)	Short Dense Coat Gasmask, Camera Lens	Fire Engine, Firefighting Equipment Bristles of Various Colors, Hair	Koala, Small Pointed Snout	Handle on Drawers, Lock on Cabinet Bathroom, Tap Fixtures	Bed, Bedroom Short Dense Coat, Dark Facial Marking
CLIP-Dissect	Dog, Cooper	Brush, Defence	Australia, Australian	Toilet, Yellow	Bedroom, Bed
WWW	Dog, Sunglasses	Watercolor, Truck	Body, Gray	Blue, Straw	Bed, Bedroom

Figure 4. Functional descriptions of penultimate-layer neurons in ResNet-50 and ViT-B/16, generated by SIEVE, CLIP-Dissect [22] and WWW [1]. SIEVE provides more complete and accurate semantic explanations. It captures localized features and multiple concepts, rather than only broad attributes such as object category or color. For example, ViT-B/16 neuron 37 is described by SIEVE with specific cues like Short Dense Coat, whereas CLIP-Dissect and WWW may omit some relevant concepts or provide only coarse labels such as Dog. Overall, the neuron-level characterizations produced by SIEVE are more fine-grained and validated.

score between cluster $C_{i,j}$ and concept t_q is represented by the average similarity:

$$g(t_q, C_{i,j}) = \frac{1}{|C_{i,j}|} \sum_{x_p \in C_{i,j}} s(x_p, t_q) \quad (2)$$

Concepts with high scores are selected as the functional hypothesis of the cluster (we set $K = 2$):

$$h_{i,j} = \arg \text{top-}K(\{g(t_q, C_{i,j}) \mid t_q \in \mathcal{T}\}, K) \quad (3)$$

where $\arg \text{top-}K(\cdot, K)$ returns the top K concepts t_q with the highest scores. Thus, neuron i obtains a set of concept labels $\mathcal{H} = \{h_{i,1}, \dots, h_{i,m}\}$, where each $h_{i,j}$ represents the functional hypothesis for the neuron's j -th high-activation pattern. This mapping captures the complex functions of neurons more accurately than a single hypothesis.

3.4. Verify Hypothesized Concepts

To verify the hypothesized concepts, we introduce the Activation Rate (AR) to measure the stability of a neuron's activation on images generated from the hypothesized concepts. The core idea is as follows: if a hypothesized concept $h_{i,j}$ reflects the functionality of neuron i in cluster $C_{i,j}$, then images generated based on this concept should elicit a strong

response from neuron i . Unlike traditional destructive interventions, such as neuron ablation, we take a constructive approach to intervention: we actively generate input stimuli that align with the hypothesized concept and observe how the neuron responds, thereby assessing the consistency and reliability of the interpretation.

Hypothesis-Guided Image Generation. For each hypothesis concept $h_{i,j}$ to be verified, we use it as a textual prompt for a pretrained text-to-image generation model G (e.g., Stable Diffusion [24]). By sampling different random noise vectors, we generate a set of images independent of the probing dataset \mathcal{D}_{probe} , denoted as $\mathcal{D}_{gen}^{(i,j)} = \{G(h_{i,j}; z) \mid z \sim \mathcal{N}(0, I)\}$. These generated samples are primarily determined by the hypothesized concept $h_{i,j}$, which helps minimize potential interference from the probing data or model biases, while may still be influenced by the training data from the generative model.

Activation Consistency Measurement. After generating the verification samples, we quantify the consistency of a neuron's responses to the hypothesized concepts using the activation rate. This allows us to assess the reliability of the functional hypotheses. Specifically, for each neuron i to be verified, its activation distribution over the probing dataset \mathcal{D}_{probe} can be obtained as $\{a_i^l(x) \mid x \in \mathcal{D}_{probe}\}$. Based on

Table 1. Quantitative comparison of neuron interpretation methods of ResNet-50 pre-trained on ImageNet-1K, using the ImageNet-1K validation set as \mathcal{D}_{probe} . We evaluate the metrics proposed by CLIP-Dissect [22] in the final layer, and the mean Activation Rate in the penultimate layer. Bold numbers indicate the best results. We use the Common Words as the concept set following CLIP-Dissect.

Method	\mathcal{D}_{probe}	$\mathcal{D}_{concept}$	Final Layer		Penultimate Layer
			CLIP cos	mpnet cos	mean AR (%)
Network Dissect	Broden	Broden	0.7073	0.3256	45.01
MILAN(b)	ImageNet val	–	0.7192	0.3089	46.10
FALCON	ImageNet val	LAION-400m	0.7031	0.2193	46.32
DnD	ImageNet val	GPT-3.5 Turbo	0.7595	0.4371	51.46
CLIP-Dissect	ImageNet val	Broden (1.2k)	0.7942	0.4543	55.16
	ImageNet val	Common Words (3k)	0.7868	0.4462	57.91
WWW	ImageNet val	Broden (1.2k)	0.7792	0.4327	49.55
	ImageNet val	Common Words (3k)	0.7713	0.4463	50.23
Ours	ImageNet val	Broden (1.2k)	0.7848	0.4452	85.73
	ImageNet val	Common Words (3k)	0.7914	0.4547	86.29

Table 2. Quantitative comparison of neuron interpretation methods of ViT-B/16 pre-trained on ImageNet-1K.

Method	\mathcal{D}_{probe}	$\mathcal{D}_{concept}$	Final Layer		Penultimate Layer
			CLIP cos	mpnet cos	mean AR (%)
FALCON	ImageNet val	LAION-400m	0.7105	0.2281	45.95
DnD	ImageNet val	GPT-3.5 Turbo	0.7462	0.4354	52.47
CLIP-Dissect	ImageNet val	Broden (1.2k)	0.7651	0.4519	56.21
	ImageNet val	Common Words (3k)	0.7538	0.4437	57.70
WWW	ImageNet val	Broden (1.2k)	0.7455	0.4261	49.19
	ImageNet val	Common Words (3k)	0.7512	0.4520	51.88
Ours	ImageNet val	Broden (1.2k)	0.7742	0.4401	84.87
	ImageNet val	Common Words (3k)	0.7858	0.4340	85.24

this distribution, the activation threshold T_i (Top 1%) is determined to distinguish significant from non-significant activations. For the set of verification samples $\mathcal{D}_{gen}^{(i,j)}$ generated from the hypothesized concept $h_{i,j}$, the Activation Rate of neuron i is defined as:

$$AR_i = \frac{1}{|\mathcal{D}_{gen}^{(i,j)}|} \sum_{x_{gen} \in \mathcal{D}_{gen}^{(i,j)}} 1\{a_i^l(x_{gen}) > T_i\}, \quad (4)$$

where $a_i^l(x_{gen})$ denotes the activation value of neuron i for the generated image x_{gen} , and $1\{\cdot\}$ is the indicator function. This metric measures the proportion of generated images, relevant to the neuron’s functional hypothesis, that elicit significant activation, reflecting the stability and consistency of the hypothesized function. After computing the Activation Rate for each neuron, we calculate the overall mean to obtain the global consistency, referred to as the mean Activation Rate. The initial mean Activation Rate is used as a filtering criterion, where hypotheses below this value are discarded, and the mean is recomputed over the retained set. This metric quantifies the alignment between the

neuron’s functional interpretations provided by the explanation method and the neuron’s true functionality, and can be used to evaluate the quality of the explanation method.

4. Experiment

We conduct extensive experiments to evaluate the proposed framework. Sec. 4.1 and Sec. 4.2 present the results from qualitative and quantitative perspectives, respectively; Sec. 4.3 assesses the contribution of each component of the framework through ablation studies; Sec. 4.4 investigates the effect of the threshold β on the framework; and Sec. 4.5 discusses the impact of domain shift on mean AR. Our evaluation covers a variety of models, including ResNet-18 [9], ResNet-50 [9], and ViT-B/16 [8]. To ensure both coverage and comparability, we adopt the concept set $\mathcal{D}_{concept}$ from CLIP-Dissect [22] and DEAL [13]. The analysis focuses on penultimate layer features of the networks, as they capture high-level semantic representations that are more likely to align with human-interpretable concepts [11].

Table 3. Quantitative comparison of neuron interpretation methods of ResNet-18 pre-trained on Places365, using the Places365 test set as \mathcal{D}_{probe} . We evaluate the metrics proposed by CLIP-Dissect [22] in the final layer, and the mean Activation Rate in the penultimate layer. Bold numbers indicate the best scores under the same settings.

Method	\mathcal{D}_{probe}	$\mathcal{D}_{concept}$	Final Layer		Penultimate Layer
			CLIP cos	mpnet cos	mean AR (%)
FALCON DnD	ImageNet val	LAION-400m	0.6975	0.2203	47.15
	Places365 test	GPT-3.5 Turbo	0.7458	0.4419	53.12
CLIP-Dissect	Places365 test	Broden (1.2k)	0.7761	0.4462	58.32
	Places365 test	Common Words (3k)	0.7883	0.4528	56.90
WWW	Places365 test	Broden (1.2k)	0.7617	0.4587	52.23
	Places365 test	Common Words (3k)	0.7526	0.4287	46.79
Ours	Places365 test	Broden (1.2k)	0.7936	0.4453	85.82
	Places365 test	Common Words (3k)	0.7833	0.4355	84.40

4.1. Qualitative Results

We qualitatively evaluated the effectiveness of SIEVE in providing neuron-level concept interpretations, focusing on the penultimate layer neurons of two representative architectures: ResNet-50 and ViT-B/16. For each neuron, we present its most highly activated images alongside textual concept explanations generated by SIEVE, CLIP-Dissect, and WWW, as illustrated in Fig. 4. In general, SIEVE demonstrates greater alignment and granularity in concept interpretation, producing descriptions that are closely aligned with neuron activations and capable of capturing local features and diverse patterns. In contrast, baselines often yield coarse or incorrect labels. SIEVE generates rich and precise concepts across different architectures. For instance, for Neuron 361 in ViT-B/16, SIEVE offers two distinct descriptions, whereas baseline methods capture only one. In particular, SIEVE focuses on common features across highly activated images, such as “Bristles of Various Colors”, while baseline methods tend to assign more specific object categories, such as “Brush”. This suggests that SIEVE can provide detailed and trustworthy insights into neuron behavior.

4.2. Quantitative Results

We evaluate the performance of the proposed method compared with baselines through quantitative experiments. Following the metrics introduced by CLIP-Dissect [22], we measure the effectiveness of a method by computing the similarity between each neuron’s hypothesized concept in the final layer and ground-truth labels. However, these metrics only capture the consistency between the functional descriptions of neurons in the final layer and ground-truth labels. They cannot assess the accuracy of neuron function descriptions in the penultimate layer. To this end, we use the mean Activation Rate, which does not rely on ground-truth labels and quantifies the consistency between a neuron’s functional description produced by an interpretability

method and the actual function of the neuron, enabling the evaluation of neuron functions beyond the final layer.

We conducted quantitative experiments on ImageNet-pretrained ResNet-50 and ViT-B/16 models, comparing our approach with Network Dissection, CLIP-Dissect [22], MILAN(b) [10], FALCON [11], WWW [1] and DnD [2]. As shown in Tab. 1 and Tab. 2, we report two metrics proposed by CLIP-Dissect as well as the mean Activation Rate. Results show that our method achieves the best or second-best performance in most cases. Specifically, on both ResNet-50 and ViT-B/16, our approach outperforms baselines in CLIP and MPNet similarity, indicating more accurate concept descriptions. More importantly, our method shows a clear advantage on the mean Activation Rate, further validating that the “Select–Hypothesize–Verify” framework generates neuron concepts with high semantic relevance. To evaluate the generalizability of our method, we tested it on ResNet-18 pretrained in Places365 (Tab. 3), showing that our approach consistently achieves top performance even on a different dataset.

4.3. Ablation Study

To verify the necessity of each component in our framework, we conduct an ablation study using the ResNet-50 pretrained on ImageNet. The baseline does not apply the activation threshold β , clustering, or concept verification. As shown in Tab. 4, the Verify module has the greatest impact, indicating that validating neuron–concept hypotheses is crucial for ensuring a reliable semantic interpretation. Select improves the consistency of interpretations by selecting samples that contribute stable and discriminative neuron activations, effectively filtering out less informative or ambiguous cases. Clustering may serve a similar purpose to selection. Once all the components have been brought together, the framework achieves the greatest possible alignment across all the metrics, thereby demonstrating the complementary effects of selection, clustering, and verification.

Table 4. Ablation study on Select, Cluster, and Verify components. Results show that all modules contribute positively to interpretation quality, with the full framework achieving the best performance across CLIP cos, mpnet cos and mean Activation Rate.

Select	Cluster	Verify	Final Layer		Penultimate Layer
			CLIP cos	mpnet cos	mean AR (%)
	✓	✓	0.6738	0.2306	45.57
	✓		0.7624	0.4301	77.90
✓		✓	0.7821	0.4423	81.52
✓	✓		0.7656	0.4189	72.87
✓	✓	✓	0.7914	0.4547	86.29

4.4. Activation Threshold Analysis

In our framework, when selecting high-activation samples, we take into account not only the magnitude of individual activations but also their ratio relative to the median of the neuron’s overall activation distribution. Some samples, even though they rank among the top activations, have a low ratio relative to this median, which suggests that the neuron lacks a clear activation preference. The hyperparameter β helps reduce the number of samples to be processed, thereby focusing on those that provide discriminative information for interpretation. Experiments were conducted using the ResNet-50 model pretrained on ImageNet. As shown in Tab. 5, varying β has minimal impact on the final interpretability metrics, since the most semantically informative samples are consistently retained. The β can be used to control sample quality without compromising the reliability of neuron-level semantic interpretations.

Table 5. Performance under different activation thresholds β . The model achieves the best results at 10, which is therefore adopted throughout the experiments in this paper.

β	Final Layer		Penultimate Layer
	CLIP cos	mpnet cos	mean AR (%)
4	0.7932	0.4421	86.05
6	0.7987	0.4517	85.61
8	0.7805	0.4432	85.72
10	0.7914	0.4547	86.29
12	0.7821	0.4478	85.98

4.5. Discussion

To quantify the effect of the domain shift, the ResNet-18 trained on remote sensing data is introduced. As shown in Tab. 6, all methods exhibit degraded results due to the impact of domain shift on the hypothesis and verification. But the verification can keep positive gains under domain shift, mitigating the impact on the hypothesis. The original and generated images are shown in Fig. 5. The significant visual discrepancy in perspective and texture between the aerial

Table 6. Performance under domain shift. Eurosat represents a distribution significantly different from the generative model’s training data, while Places365 represents a general domain.

Method	Eurosat (domain shift)		Places365 (general)	
	CLIP cos	mean AR (%)	CLIP cos	mean AR (%)
CLIP-Dis.	0.7152	43.16	0.7883	56.90
WWW	0.7047	37.43	0.7526	46.79
Ours	0.7393	75.45	0.7833	84.40



Figure 5. Visualization of the domain shift effect. Significant discrepancies exist between aerial and generated samples.

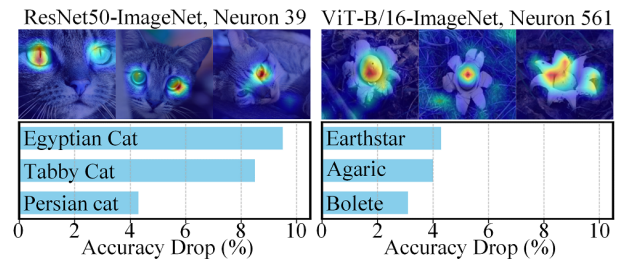


Figure 6. The heatmap (top) shows the part of the image that activates Neuron 39 the most, which is the cat’s eyes. The bar plot (bottom) quantifies the ablation effect, showing a targeted accuracy drop for semantically related feline categories.

view (left) and the generated images (right) intuitively illustrates the challenge introduced by the domain shift. Beyond domain shift, we explore how individual neuron aligns with specific concepts. We ablate individual neurons to measure class-specific accuracy drops. As shown in Fig. 6, Neuron 39 in ResNet-50 primarily responds to cat eyes, and ablating it predominantly degrades accuracy for feline categories. A similar pattern is observed in ViT-B/16.

5. Conclusion

This work focuses on addressing the limitations of current methods, which are limited by the two assumptions: 1) assuming that each neuron can capture discriminative features; and 2) assuming that each concept generated by models is accurate. To address both issues, we propose a Select–Hypothesize–Verify framework for interpreting neuron functionality (dubbed SIEVE), which both filters out low-discriminatory neurons and enables closed-loop verification on neuron concepts to avoid mismatched concepts.

Acknowledgements

This work was supported in part by the National Science Foundation of China Joint Key Project under Grant U24B20173, U24B20182, and by the National Natural Science Foundation of China under Grant 62576060, 62536002, 62561160098.

References

- [1] Yong Hyun Ahn, Hyeon Bae Kim, and Seong Tae Kim. Www: a unified framework for explaining what where and why of neural networks by interpretation of neuron concepts. In *Proceedings of the IEEE/CVF Conference on Computer Vision and Pattern Recognition*, pages 10968–10977, 2024. 2, 5, 7
- [2] Nicholas Bai, Rahul Iyer, Tuomas Oikarinen, Akshay Kulkarini, and Tsui-Wei Weng. Interpreting neurons in deep vision networks with language models. *Transactions on Machine Learning Research*, 2025. 2, 3, 7
- [3] David Bau, Bolei Zhou, Aditya Khosla, Aude Oliva, and Antonio Torralba. Network dissection: Quantifying interpretability of deep visual representations. In *Proceedings of the IEEE conference on computer vision and pattern recognition*, pages 6541–6549, 2017. 2, 3
- [4] David Bau, Jun-Yan Zhu, Hendrik Strobelt, Agata Lapedriza, Bolei Zhou, and Antonio Torralba. Understanding the role of individual units in a deep neural network. *Proceedings of the National Academy of Sciences*, 117(48):30071–30078, 2020. 3
- [5] Steven Bills, Nick Cammarata, Dan Mossing, Henk Tillman, Leo Gao, Gabriel Goh, Ilya Sutskever, Jan Leike, Jeff Wu, and William Saunders. Language models can explain neurons in language models. <https://openaipublic.blob.core.windows.net/neuron-explainer/paper/index.html>, 2023. 3
- [6] Fahim Dalvi, Hassan Sajjad, Nadir Durrani, and Yonatan Belinkov. Analyzing redundancy in pretrained transformer models. In *2020 Conference on Empirical Methods in Natural Language Processing, EMNLP 2020*, pages 4908–4926. Association for Computational Linguistics (ACL), 2020. 2
- [7] Finale Doshi-Velez and Been Kim. Towards a rigorous science of interpretable machine learning. *stat*, 1050:2, 2017. 2
- [8] Alexey Dosovitskiy. An image is worth 16x16 words: Transformers for image recognition at scale. *arXiv preprint arXiv:2010.11929*, 2020. 6
- [9] Kaiming He, Xiangyu Zhang, Shaoqing Ren, and Jian Sun. Identity mappings in deep residual networks. In *European conference on computer vision*, pages 630–645. Springer, 2016. 6
- [10] Evan Hernandez, Sarah Schwettmann, David Bau, Teona Bagashvili, Antonio Torralba, and Jacob Andreas. Natural language descriptions of deep visual features. In *International Conference on Learning Representations*, 2021. 3, 7
- [11] Neha Kalibhat, Shweta Bhardwaj, C Bayan Bruss, Hamed Firooz, Maziar Sanjabi, and Soheil Feizi. Identifying interpretable subspaces in image representations. In *International Conference on Machine Learning*, pages 15623–15638. PMLR, 2023. 2, 3, 6, 7
- [12] Biagio La Rosa, Leilani Gilpin, and Roberto Capobianco. Towards a fuller understanding of neurons with clustered compositional explanations. *Advances in Neural Information Processing Systems*, 36:70333–70354, 2023. 3
- [13] Tang Li, Mengmeng Ma, and Xi Peng. Deal: Disentangle and localize concept-level explanations for vlms. In *European Conference on Computer Vision*, pages 383–401. Springer, 2024. 6
- [14] Aravindh Mahendran and Andrea Vedaldi. Understanding deep image representations by inverting them. In *Proceedings of the IEEE conference on computer vision and pattern recognition*, pages 5188–5196, 2015. 2
- [15] Ari S Morcos, David GT Barrett, Neil C Rabinowitz, and Matthew Botvinick. On the importance of single directions for generalization. In *International Conference on Learning Representations*, 2018. 3
- [16] Alexander Mordvintsev, Christopher Olah, and Mike Tyka. Deepdream-a code example for visualizing neural networks. *Google Research*, 2(5):67, 2015. 3
- [17] Jesse Mu and Jacob Andreas. Compositional explanations of neurons. *Advances in Neural Information Processing Systems*, 33:17153–17163, 2020. 2
- [18] Fionn Murtagh and Pierre Legendre. Ward’s hierarchical agglomerative clustering method: which algorithms implement ward’s criterion? *Journal of classification*, 31(3):274–295, 2014. 4
- [19] Vedant Nanda, Till Speicher, John Dickerson, Krishna Gumjadi, Soheil Feizi, and Adrian Weller. Diffused redundancy in pre-trained representations. *Advances in Neural Information Processing Systems*, 36:4055–4079, 2023. 2
- [20] Anh Nguyen, Alexey Dosovitskiy, Jason Yosinski, Thomas Brox, and Jeff Clune. Synthesizing the preferred inputs for neurons in neural networks via deep generator networks. *Advances in neural information processing systems*, 29, 2016. 3
- [21] Tuomas Oikarinen and Tsui-Wei Weng. Linear explanations for individual neurons. In *Proceedings of the 41st International Conference on Machine Learning*, pages 38639–38662, 2024. 3
- [22] Tuomas P. Oikarinen and Tsui-Wei Weng. Clip-dissect: Automatic description of neuron representations in deep vision networks. In *The Eleventh International Conference on Learning Representations, ICLR 2023, Kigali, Rwanda, May 1-5, 2023*. OpenReview.net, 2023. 2, 3, 4, 5, 6, 7
- [23] Chris Olah, Alexander Mordvintsev, and Ludwig Schubert. Feature visualization. *Distill*, 2(11):e7, 2017. 2, 3
- [24] Dustin Podell, Zion English, Kyle Lacey, Andreas Blattmann, Tim Dockhorn, Jonas Müller, Joe Penna, and Robin Rombach. SDXL: improving latent diffusion models for high-resolution image synthesis. In *The Twelfth International Conference on Learning Representations, ICLR 2024, Vienna, Austria, May 7-11, 2024*. OpenReview.net, 2024. 5
- [25] Henri Poincaré. Science and method. 1914. 2
- [26] Karl R Popper. The logic of scientific discovery. 1959. 2

- [27] Alec Radford, Jong Wook Kim, Chris Hallacy, Aditya Ramesh, Gabriel Goh, Sandhini Agarwal, Girish Sastry, Amanda Askell, Pamela Mishkin, Jack Clark, et al. Learning transferable visual models from natural language supervision. In *International conference on machine learning*, pages 8748–8763. PmLR, 2021. [2](#)
- [28] Marco Tulio Ribeiro, Sameer Singh, and Carlos Guestrin. ” why should i trust you?” explaining the predictions of any classifier. In *Proceedings of the 22nd ACM SIGKDD international conference on knowledge discovery and data mining*, pages 1135–1144, 2016. [3](#)
- [29] Peter J Rousseeuw. Silhouettes: a graphical aid to the interpretation and validation of cluster analysis. *Journal of computational and applied mathematics*, 20:53–65, 1987. [4](#)
- [30] Ramprasaath R Selvaraju, Michael Cogswell, Abhishek Das, Ramakrishna Vedantam, Devi Parikh, and Dhruv Batra. Grad-cam: Visual explanations from deep networks via gradient-based localization. In *Proceedings of the IEEE international conference on computer vision*, pages 618–626, 2017. [2](#)
- [31] Tamar Rott Shaham, Sarah Schwettmann, Franklin Wang, Achyuta Rajaram, Evan Hernandez, Jacob Andreas, and Antonio Torralba. A multimodal automated interpretability agent. In *Forty-first International Conference on Machine Learning*, 2024. [3](#)
- [32] Karen Simonyan, Andrea Vedaldi, and Andrew Zisserman. Deep inside convolutional networks: Visualising image classification models and saliency maps. *arXiv preprint arXiv:1312.6034*, 2013. [2](#)
- [33] Matthew D Zeiler and Rob Fergus. Visualizing and understanding convolutional networks. In *European conference on computer vision*, pages 818–833. Springer, 2014. [2](#), [3](#)
- [34] Yu Zhang, Peter Tiño, Aleš Leonardis, and Ke Tang. A survey on neural network interpretability. *IEEE transactions on emerging topics in computational intelligence*, 5(5):726–742, 2021. [2](#)
- [35] Bolei Zhou, Aditya Khosla, Agata Lapedriza, Aude Oliva, and Antonio Torralba. Learning deep features for discriminative localization. In *Proceedings of the IEEE conference on computer vision and pattern recognition*, pages 2921–2929, 2016. [2](#)